Electronic Supplementary Material (ESI) for ChemComm.

SUPPLEMENTARY INFORMATION

for

Electrochemical amphotericity and NIR absorption induced via the step-wise protonation of fused quinoxaline-tetrathiafulvalene-pyrroles

Jung Su Park,*[‡a] Trang Thu Tran,[‡a] Jongmin Kim,[b] Jonathan L. Sessler*[c].

Contents:

I. Synthesis and Characterization:

1. Synthesis of quinoxaline annulated TTF-pyrrole derivatives

Synthesis of 1

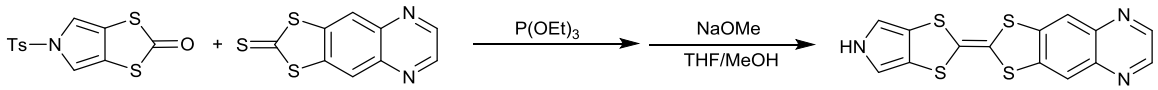

1

In accord with the scheme given above, a mixture of 5-tosyl-5H-[1,3]dithiolo[4,5-c]pyrrol-2-one (0.50 g, 1.61 mmol)[1] and [1,3]dithiolo[4,5-g]quinoxaline-2-thione[2] (0.57 g, 2.41 mmol) in 30 mL of neat triethylphosphite was stirred for 6 hours at 140 ℃ and then cooled to room temperature. Addition of 100 mL of MeOH into the reaction mixture led to precipitation of dark red solid, which was then collected by filtration. After redissolving the solid in a mixture of methanol (100 mL) and THF (100 mL), 10 equivalents of sodium methoxide (30% in MeOH) were added. The mixture was then heated to 50 ℃ for 30 minutes and poured into 100 mL of a saturated aqueous solution of NH_4Cl. After filtration and washing with water, the dark red precipitate was collected. The mixture was purified by column chromatography (silica gel, dichloromethane/hexanes = 4:1, eluent) to give **1** in the form of a red solid (0.12g, 23 %). M.p. 234-236 ℃ dec.
1: HR-ESI-MS: *m/z* calcd for $[C_{14}H_5N_3S_4]H^+$: 343.9444; found: 343.9446. ; ^{1}H NMR (500MHz, $(CD_3)_2SO$, 25^{o}C, TMS) δ[ppm]: 11.14 (s, br, 1H), 8.79 (s, 2H), 8.18 (s, 2H), 6.84 (d, 2H, 2.7Hz), ^{13}C NMR (126 MHz, $(CD_3)_2SO$, 25^{o}C, TMS) δ[ppm] : 145.4, 141.2, 140.6, 123.9, 120.8, 117.0, 110.9, 107.3.

Synthesis of 2 and 3

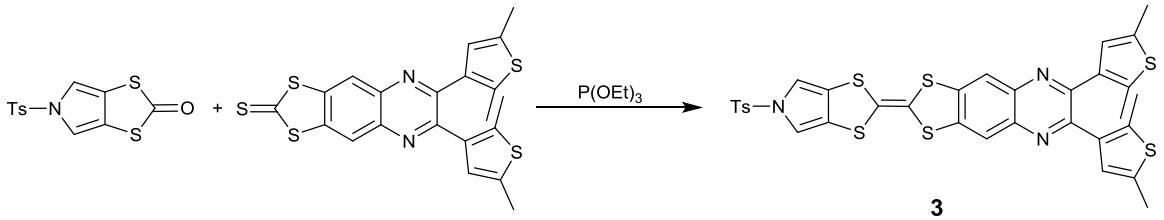

3

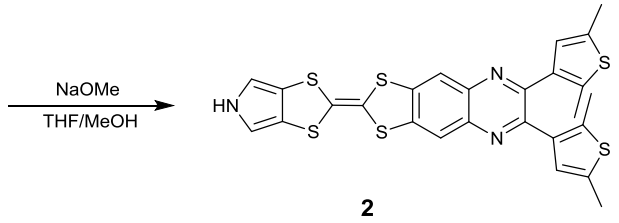

2

3: A mixture of 5-tosyl-5H-[1,3]dithiolo[4,5-c]pyrrol-2-one (0.70 g, 2.25 mmol)[1] and 6,7-bis(2,5-dimethylthiophen-3-yl)-[1,3]dithiolo[4,5-g]quinoxaline-2-thione[2] (1.54 g, 3.37 mmol) in neat triethylphosphite (40 mL) was stirred for 12 hours at 140 ℃ and then cooled to room temperature. Adding 100 mL of cold MeOH into the reaction mixture led to precipitation of an orange solid, which was collected by filtration. The collected orange solid was purified by column chromatography (silica gel, dichloromethane/hexanes = 4:1, eluent); this afforded **3** as an orange solid. M.p. 198-200 ℃ **3**: ESI-MS: *m/z* calcd for $[C_{33}H_{25}N_3O_2S_7]H^+$: 720.0070; found: 720.0083; ^{1}H NMR (500 MHz, CD_2Cl_2, 25^{o}C, TMS) δ[ppm]: 7.79 (s, 2H), 7.67 (d, 2H, 8.43 Hz), 7.26 (d, 2H, 8.07 Hz), 6.92 (s, 2H), 6.38 (d, 2H, 0.96 Hz), 2.33 (s, 3H), 2.27 (s, 6H), 2.12 (s, 6H), ^{13}C NMR (126 MHz, CD_2Cl_2, 25^{o}C, TMS) δ[ppm] : 150.3, 145.9, 140.0, 139.6, 137.5, 135.5, 135.2, 130.2, 126.9, 126.8, 126.7, 120.04, 119.9, 115.3, 111.5, 21.6, 14.6, 13.7.

2: Sodium methoxide (15 equivalents; 30% in MeOH) was added to a solution of **3** (0.30 g, 0.42 mmol) in mixture of methanol (25 mL) and THF (25 mL). The mixture was then heated to 50 ℃ for 30 minutes and poured into 100 mL of a saturated aqueous solution of NH_4Cl. After filtration and washing with water, the resulting yellow precipitate was collected and purified by column chromatography (silica gel, dichloromethane/hexanes = 4:1, eluent) to give **1** in the form of a yellow solid (0.22 g, 93 %). M.p. 248-250 ℃ dec. **2**: ESI-MS: *m/z* calcd for $[C_{26}H_{18}N_3S_6]^-$; 563.9825; found: 563.9822; ^{1}H NMR (500MHz, $(CD_3)_2SO$, 25^{o}C, TMS) δ[ppm]: 11.19 (s, 1H), 8.18 (s, 2H), 6.87 (d, 2H, 2.5 Hz), 6.52

(s, 2H), 2.33 (s, 6H), 2.15 (s, 6H, ^{13}C NMR (126 MHz, $(CD_3)_2SO$, 25^{o}C, TMS) δ[ppm] : 145.0, 140.7, 139.6, 137.1, 135.8, 135.2, 127.6, 123.9, 120.8, 117.4, 111.4, 108.0, 15.3, 14.0.

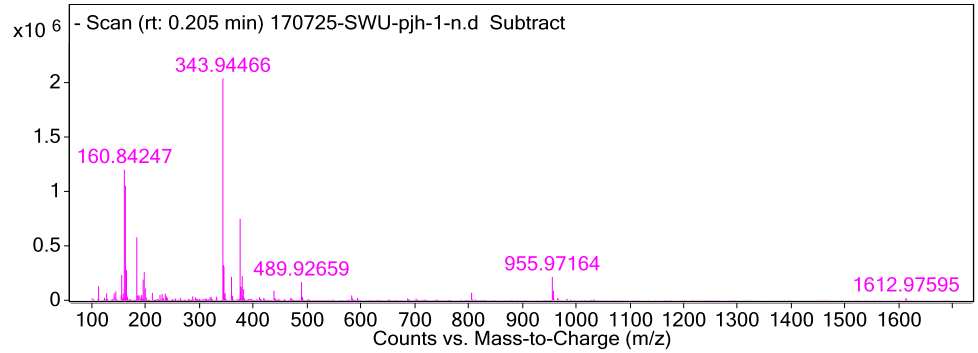

Figure S1. HR-ESI mass spectrum of **1**.

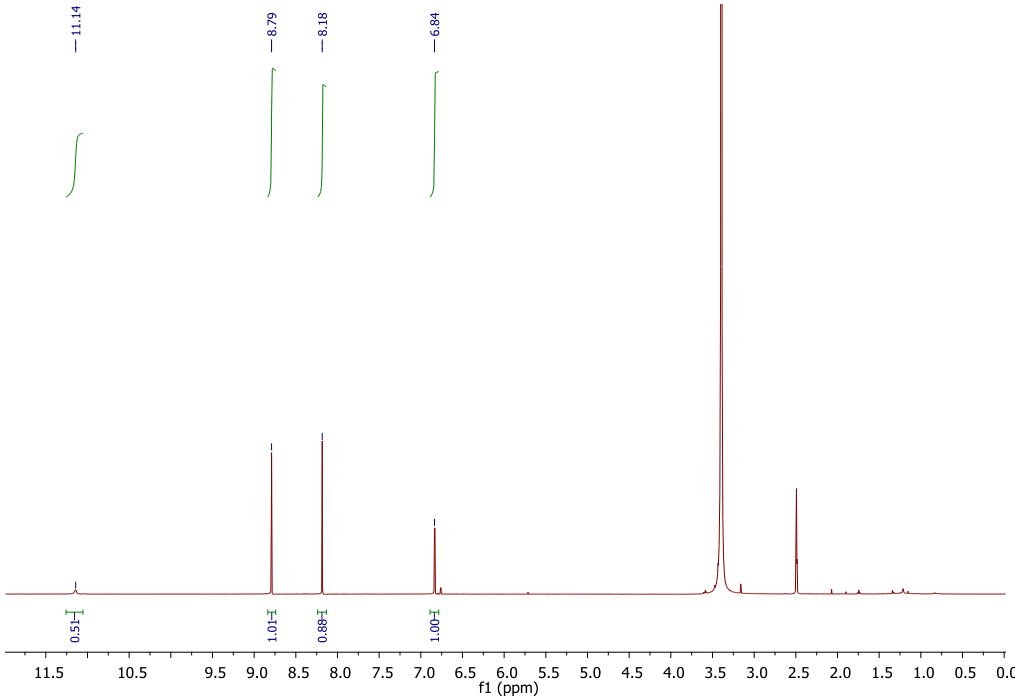

Figure S2. ^{1}H NMR spectrum of **1** recorded in $(CD_3)_2SO$ at room temperature.

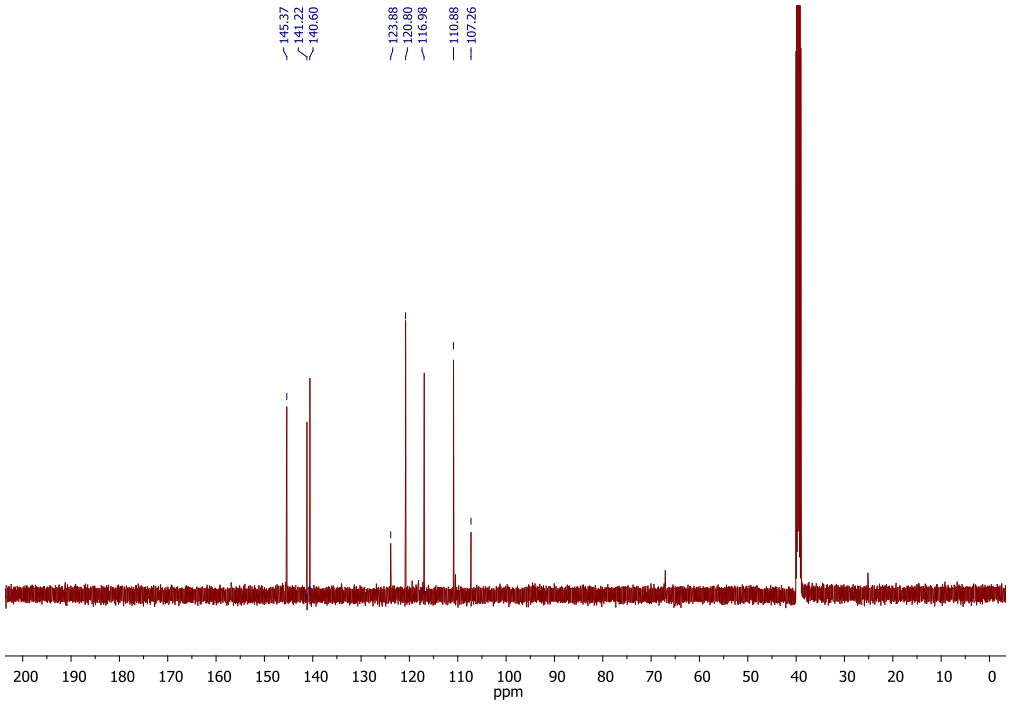

Figure S3. ^{13}C NMR spectrum of **1** recorded in $(CD_3)_2SO$ at room temperature.

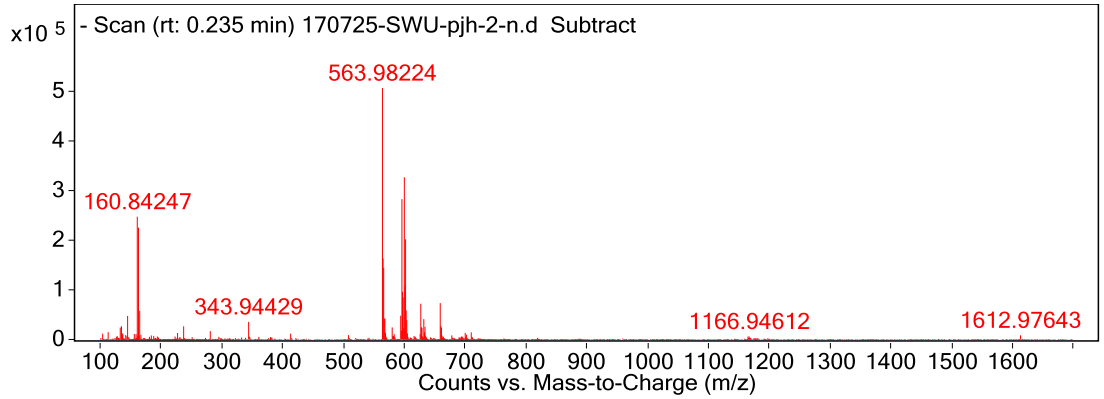

Figure S4. HR-ESI mass spectrum of **2**

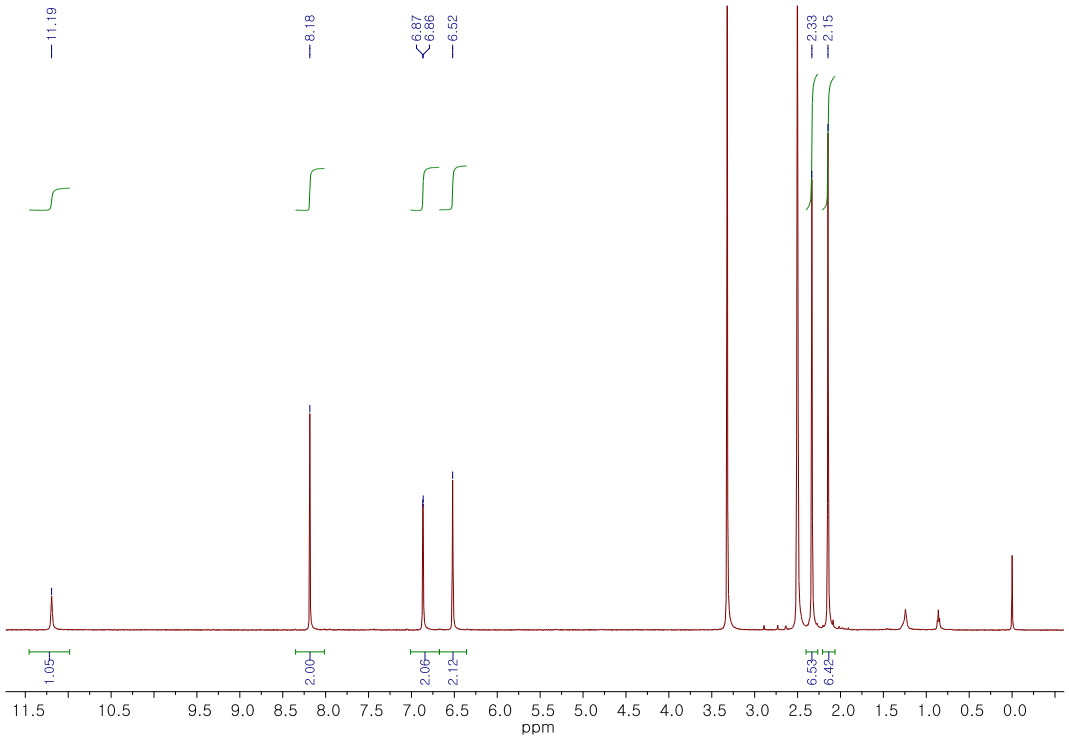

Figure S5. ^{1}H NMR spectrum of **2** recorded in $(CD_3)_2SO$.

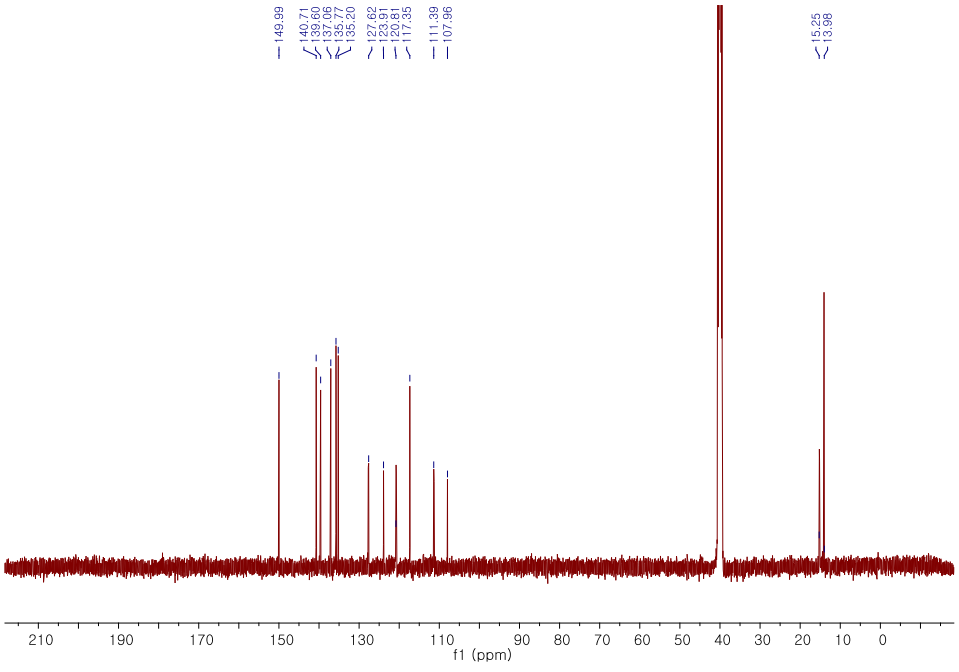

Figure S6. ^{13}C NMR spectrum of **2** recorded in $(CD_3)_2SO$.

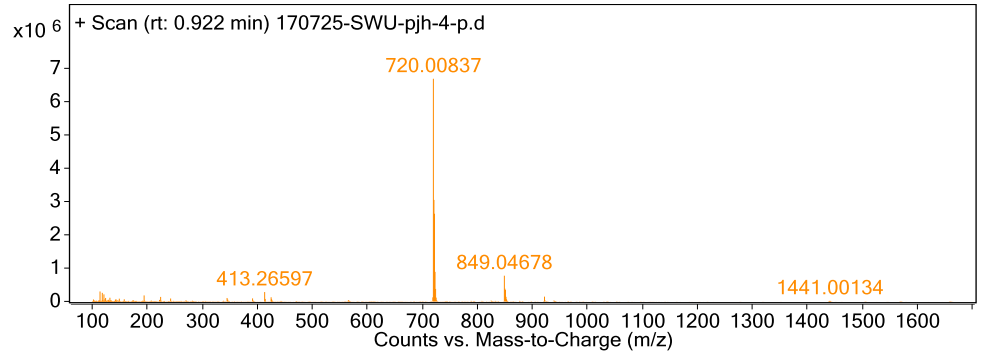

Figure S7. HR-ESI mass spectrum of **3**.

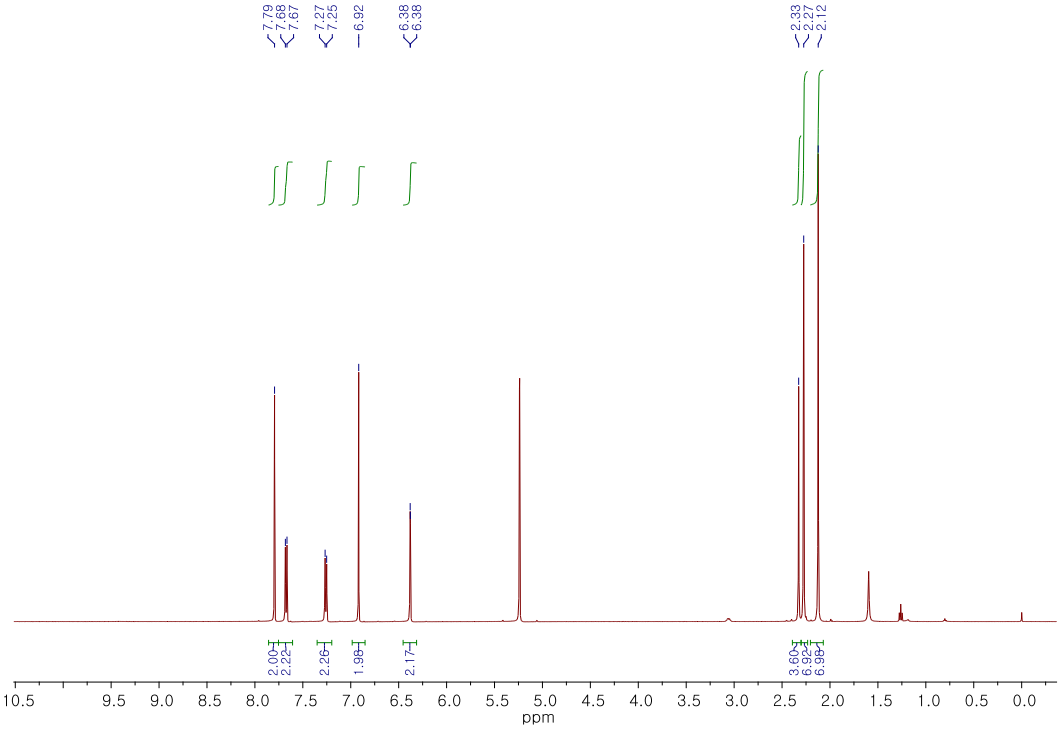

Figure S8. ^{1}H NMR spectrum of **3** recorded in CD_2Cl_2.

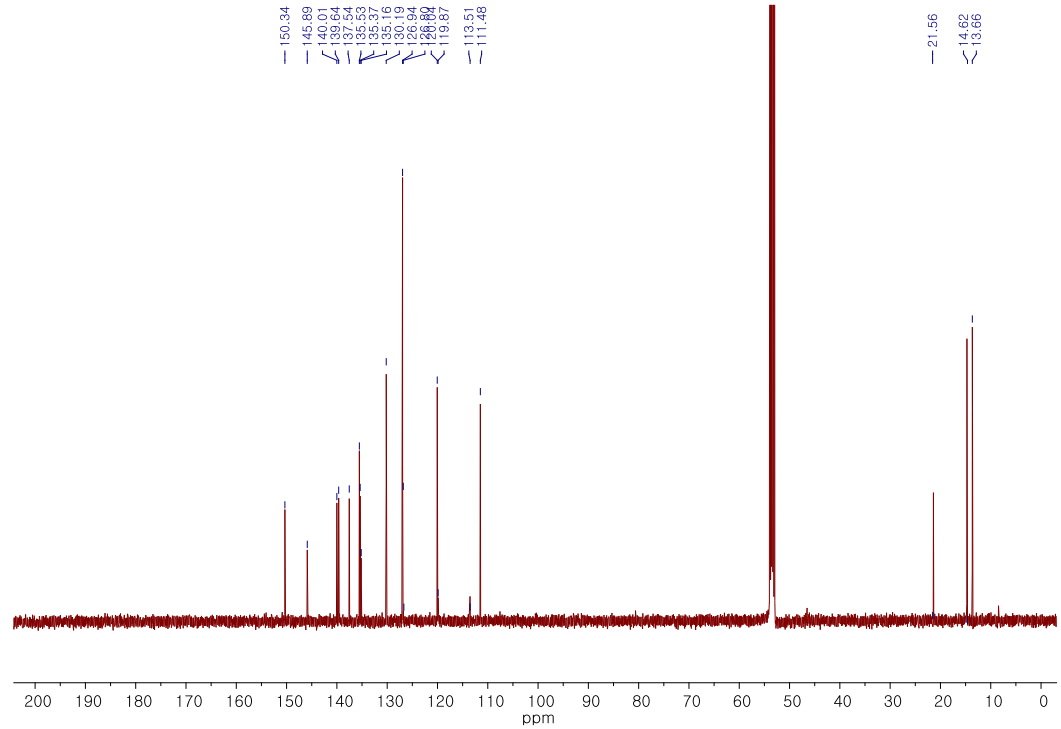

Figure S9. ^{13}C NMR spectrum of **3** recorded in CD_2Cl_2.

II. Electrochemistry

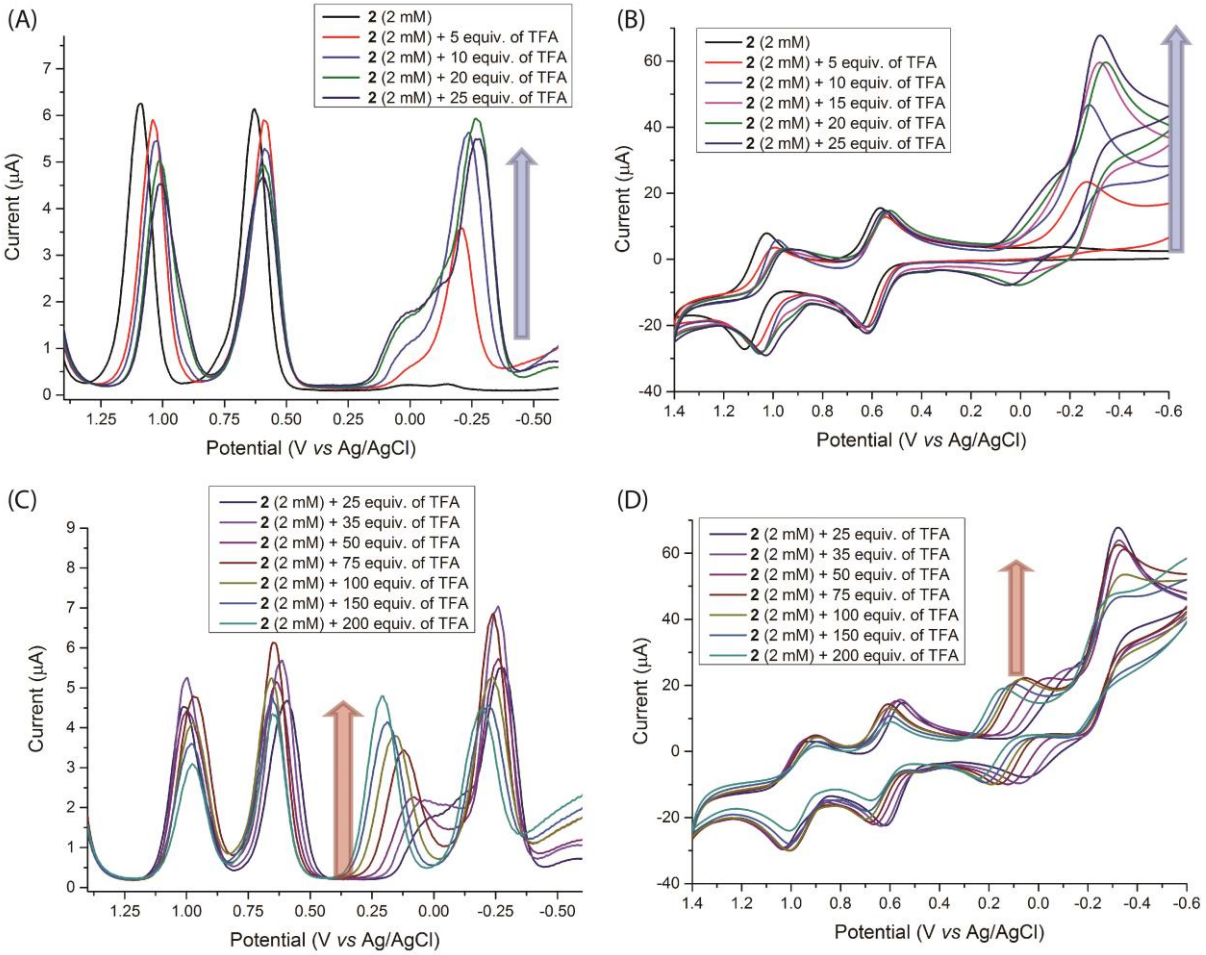

Figure S10. Changes in differential pulse voltammograms (DPVs) and cyclic-voltammograms (CVs) of 2 mM dichloromethane solutions of **2** seen upon the addition of incremental amounts of TFA in the presence of 0.5 M $TBAPF_6$. Note the two-step protonation process.

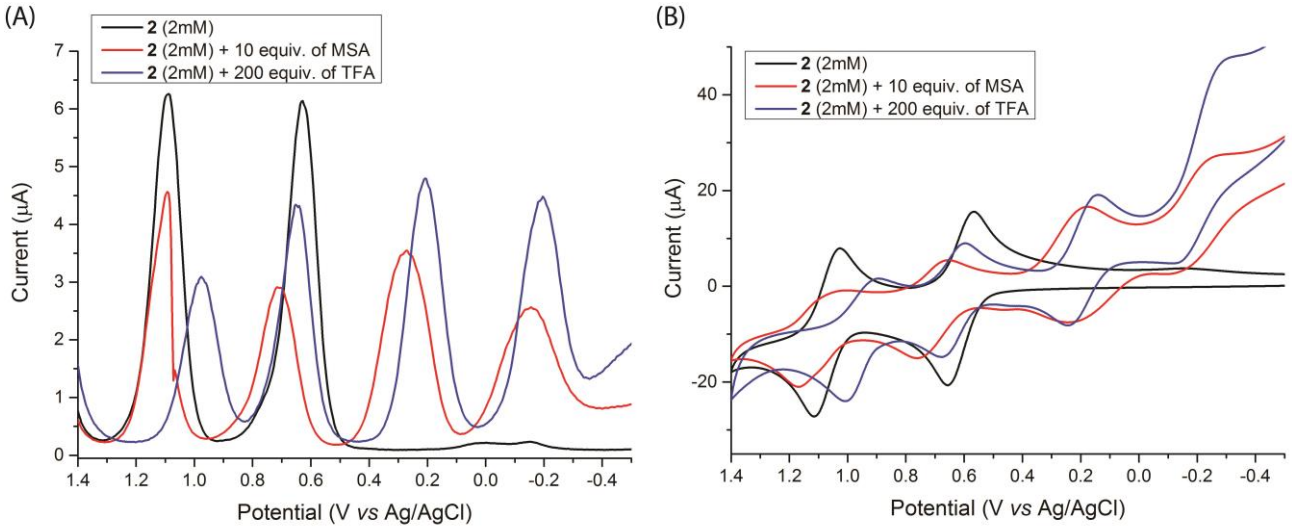

Figure S11. Comparison of differential pulse voltammograms (DPVs) and cyclic-voltammograms (CVs) of 2 mM dichloromethane solutions of **2** recorded in the presence of 10 equivalents of MSA *vs* 200 equivalents of TFA containing 0.5 M of $TBAPF_6$.

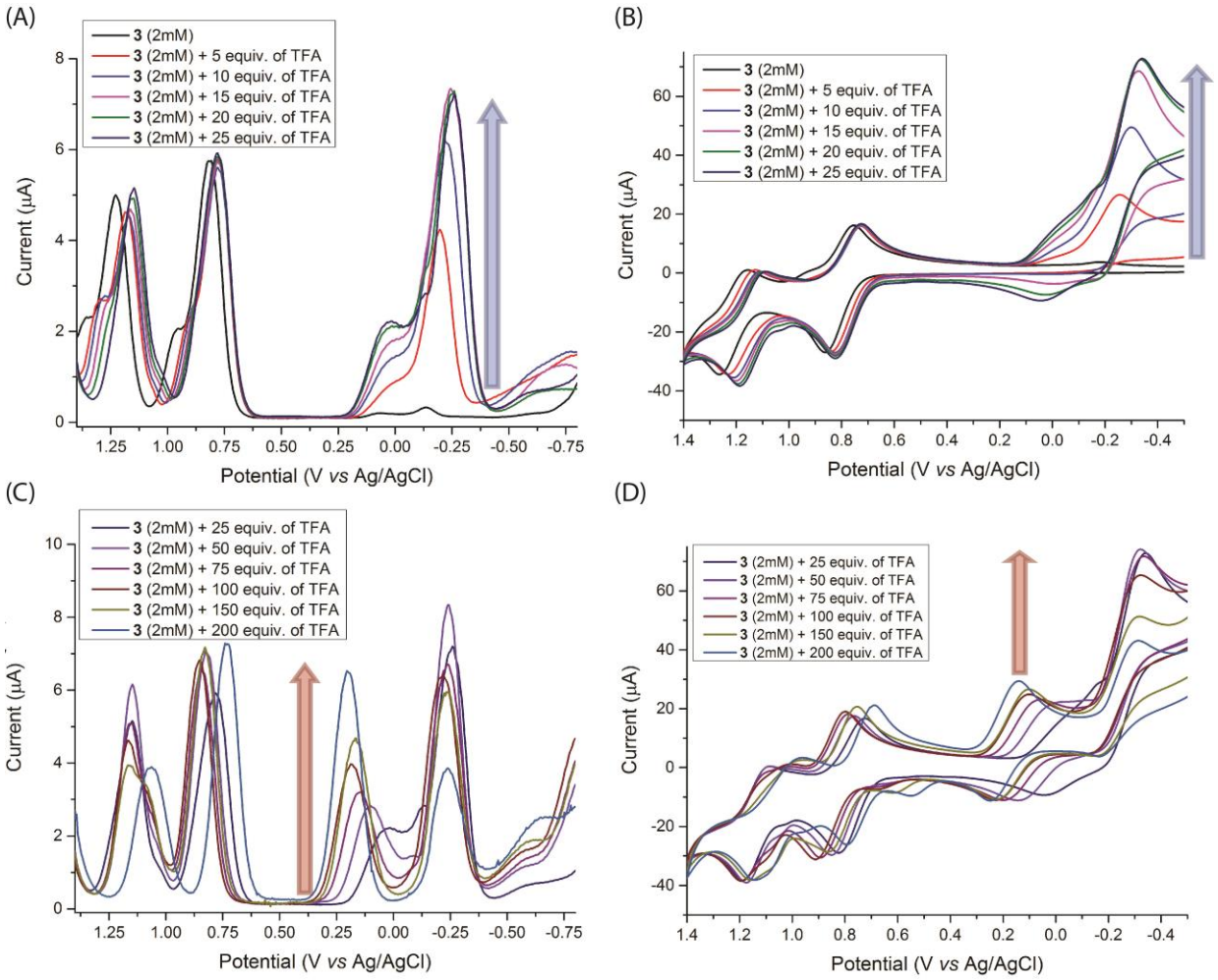

Figure S12. Changes in differential pulse voltammograms (DPVs) and cyclic-voltammograms (CVs) of 2 mM dichloromethane solutions of **3** seen upon the incremental addition of TFA in the presence of 0.5 M $TBAPF_6$. Note the two-step protonation process.

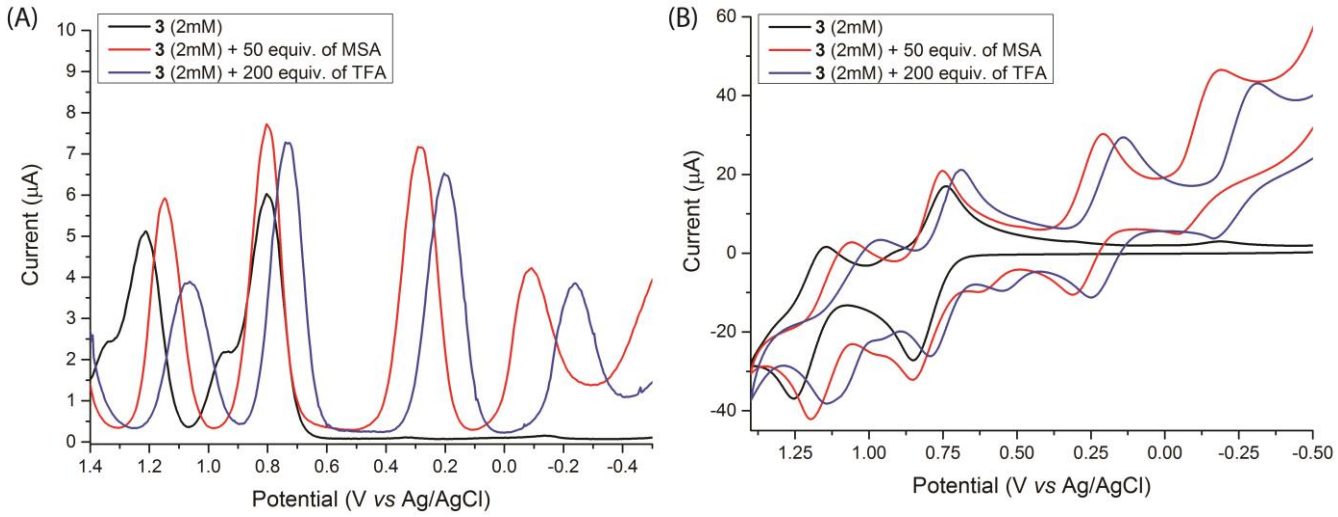

Figure S13. Comparison of differential pulse voltammograms (DPVs) and cyclic-voltammograms (CVs) of 2 mM dichloromethane solutions of **3** recorded in the presence of 10 equivalents of MSA *vs* 200 equivalents of TFA containing 0.5 M $TBAPF_6$.

III. UV-Vis-NIR Spectral Titrations:

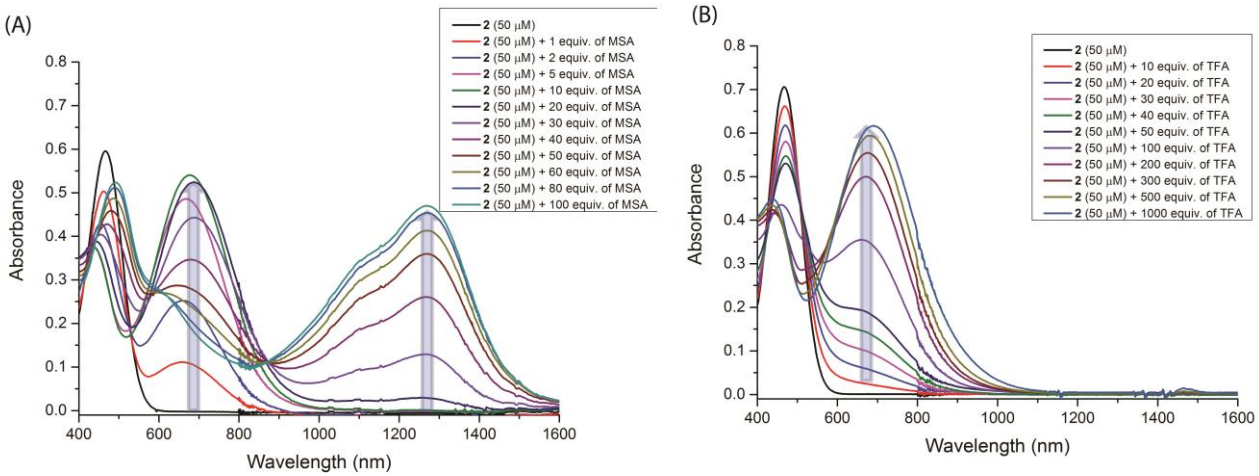

Figure S14. UV-Vis-NIR spectral changes seen for a 50 μM dichloromethane solution of **2** upon the incremental addition of MSA (left) and TFA (right).

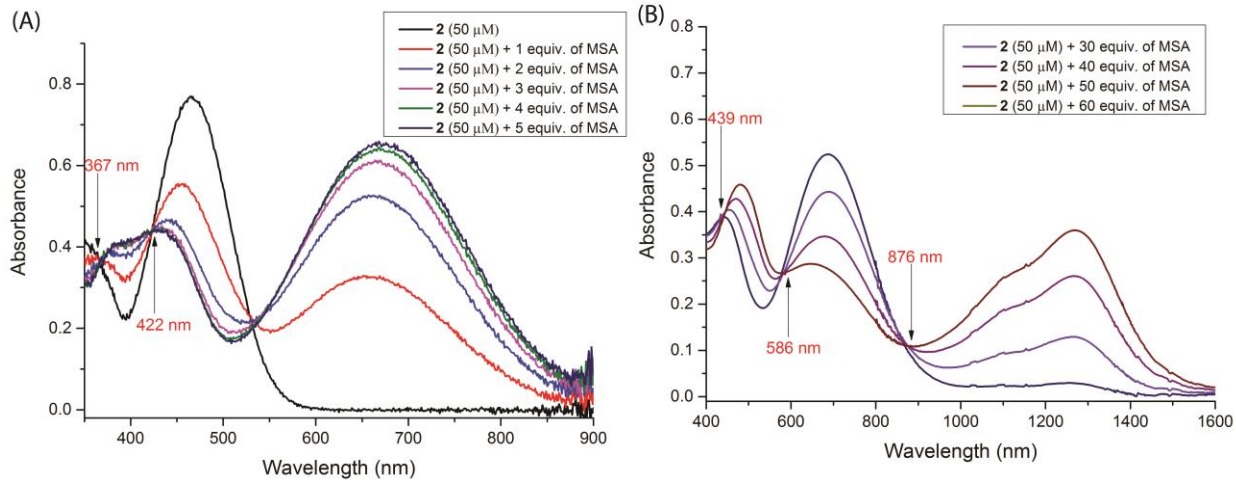

Figure S15. Stacked UV-Vis-NIR spectra of a 50 μM dichloromethane solution of **2** obtained via the incremental addition of MSA. Note the isosbestic points during the presumed mono-(left) and diprotonation (right) events.

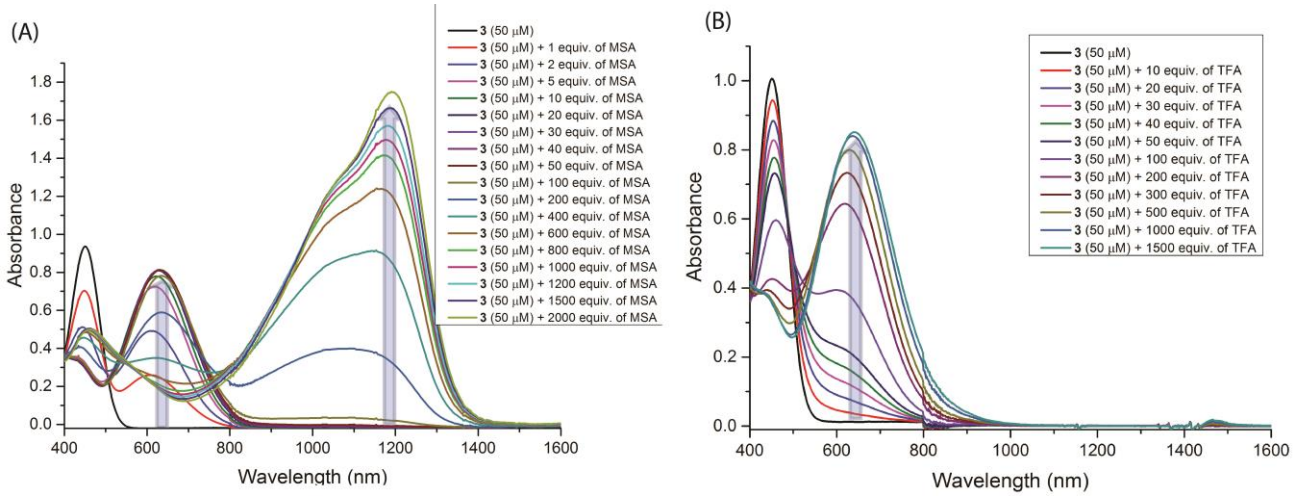

Figure S16. UV-Vis-NIR spectral changes of a 50 μM dichloromethane solution of **3** seen upon the incremental addition of MSA and TFA.

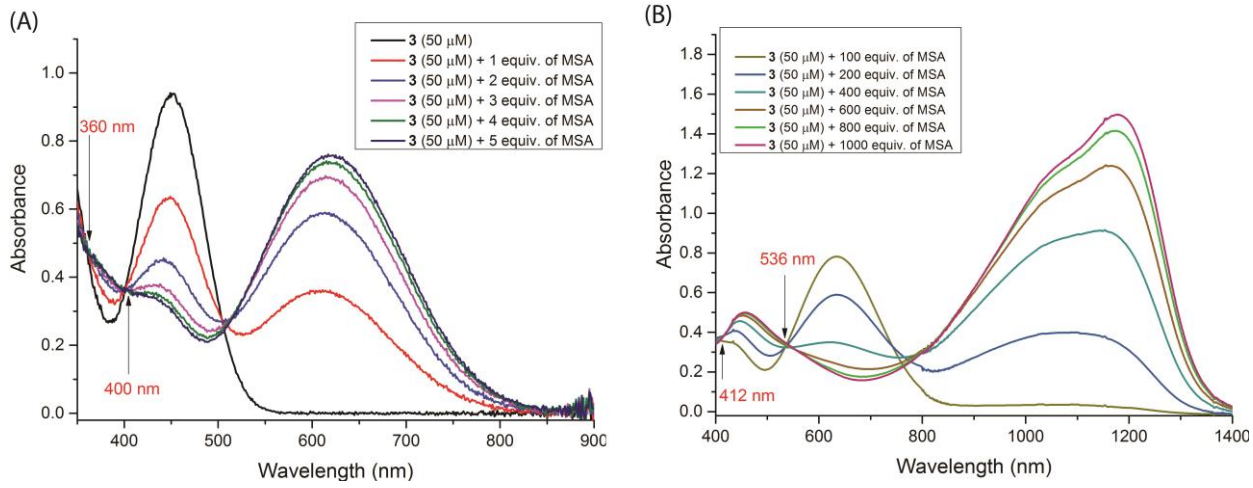

Figure S17. Stacked UV-Vis-NIR spectra of a 50 μM dichloromethane solution of **3** obtained via the incremental addition of MSA. Note the isosbestic points during the presumed mono-(left) and diprotonation (right) events.

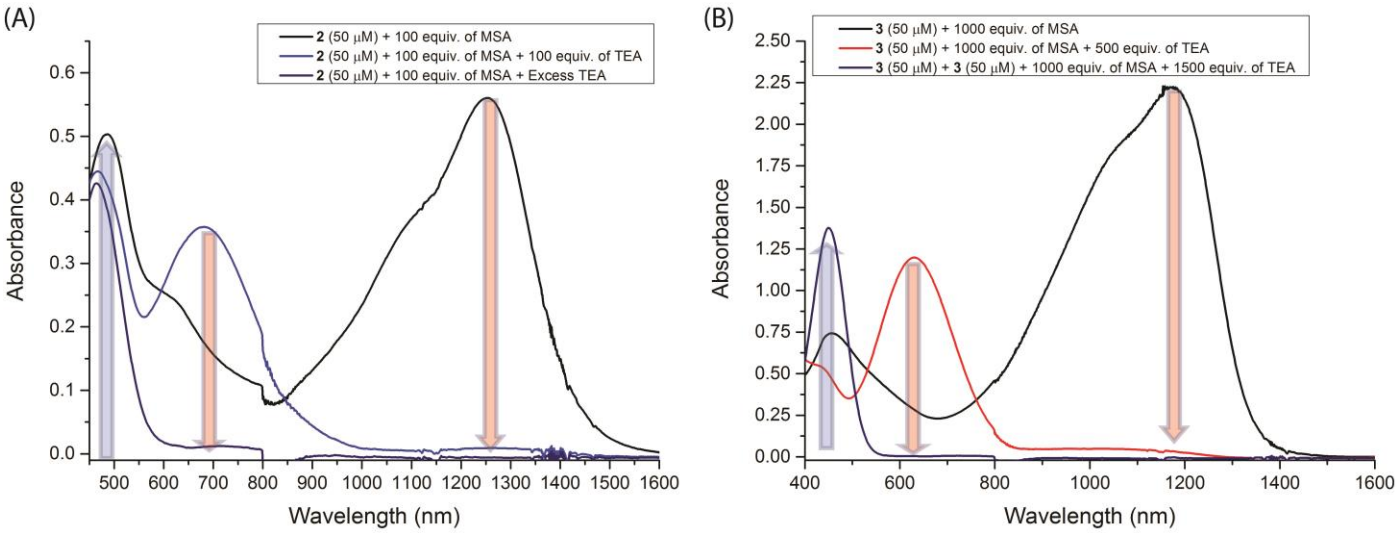

Figure S18. UV-Vis-NIR spectral changes seen for 50 μM dichloromethane solution of the diprotonated forms of **2** and **3** upon the addition of TEA. Note the changes corresponding to reversible and stepwise deprotonation events.

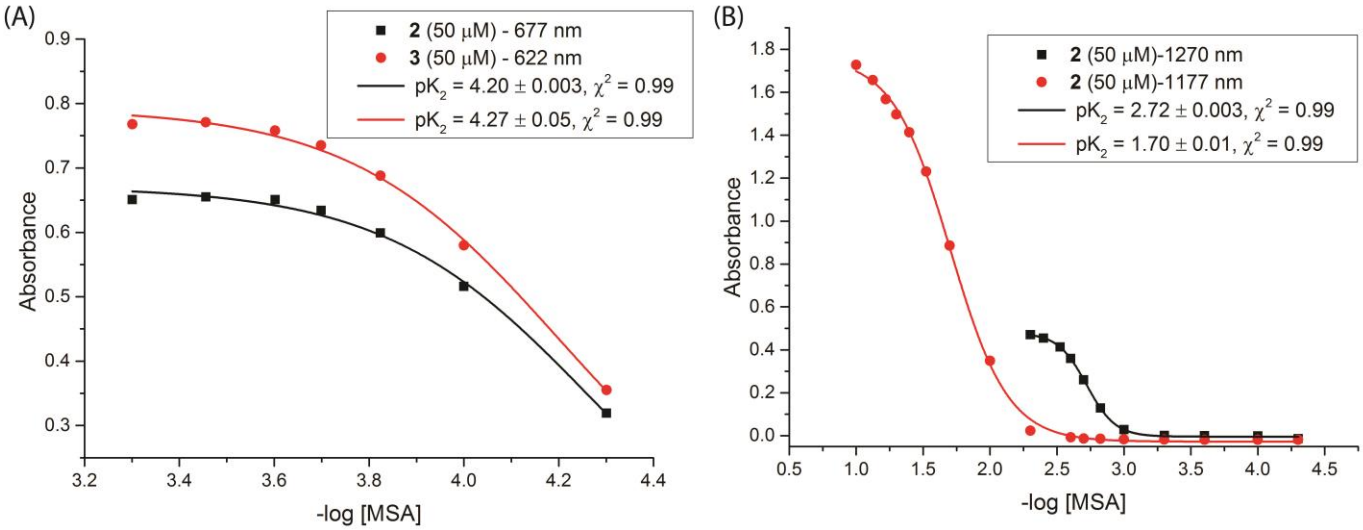

Figure S19. Plot of the absorbance change of **2** and **3** *vs.* –log [MSA] and a non-linear curvefit of the data. Note the difference in inferred pKa values.

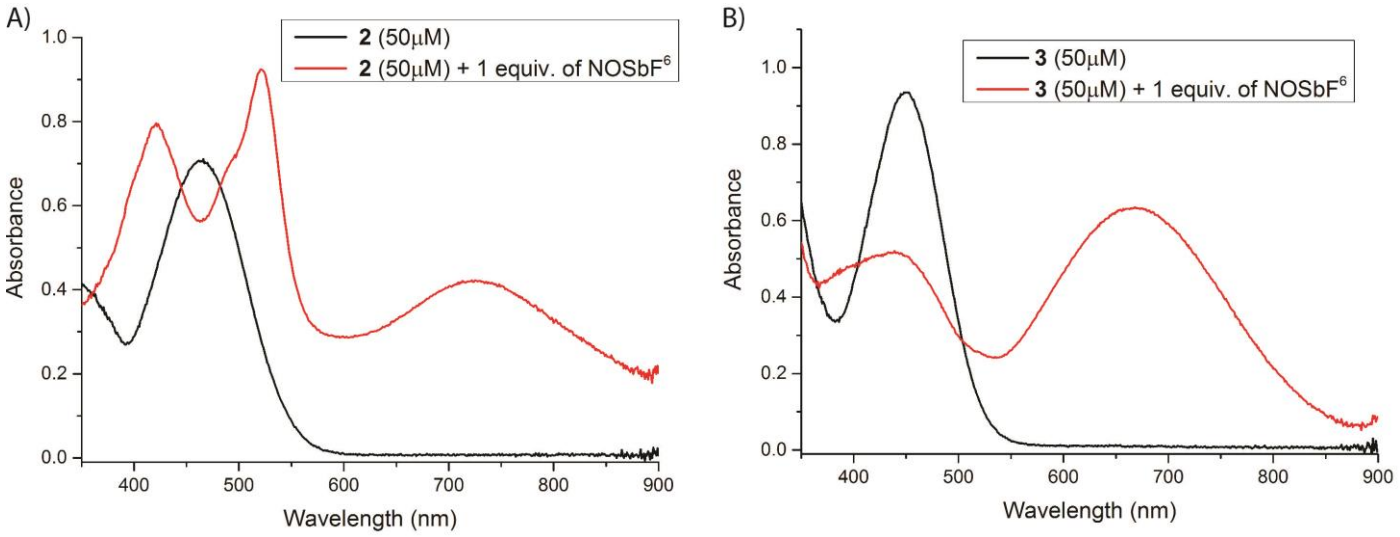

Figure S20. UV-Vis-NIR spectral changes seen for 50 μM dichloromethane solution of **2** and **3** upon the addition of 1 equivalent of $NOSbF_6$.

IV. Fluorescence Studies

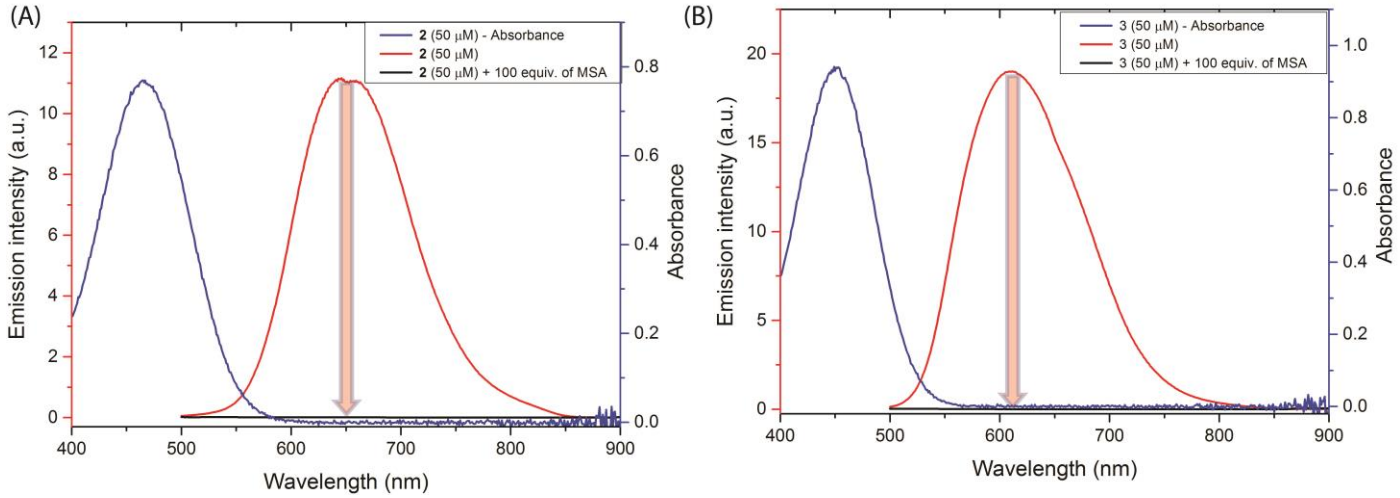

Figure S21. Change in the fluorescence emission features of 50 μM dichloromethane solutions of **2** and **3** observed upon the respective addition of 100 equivalents of MSA.

V. NMR Spectroscopic Studies

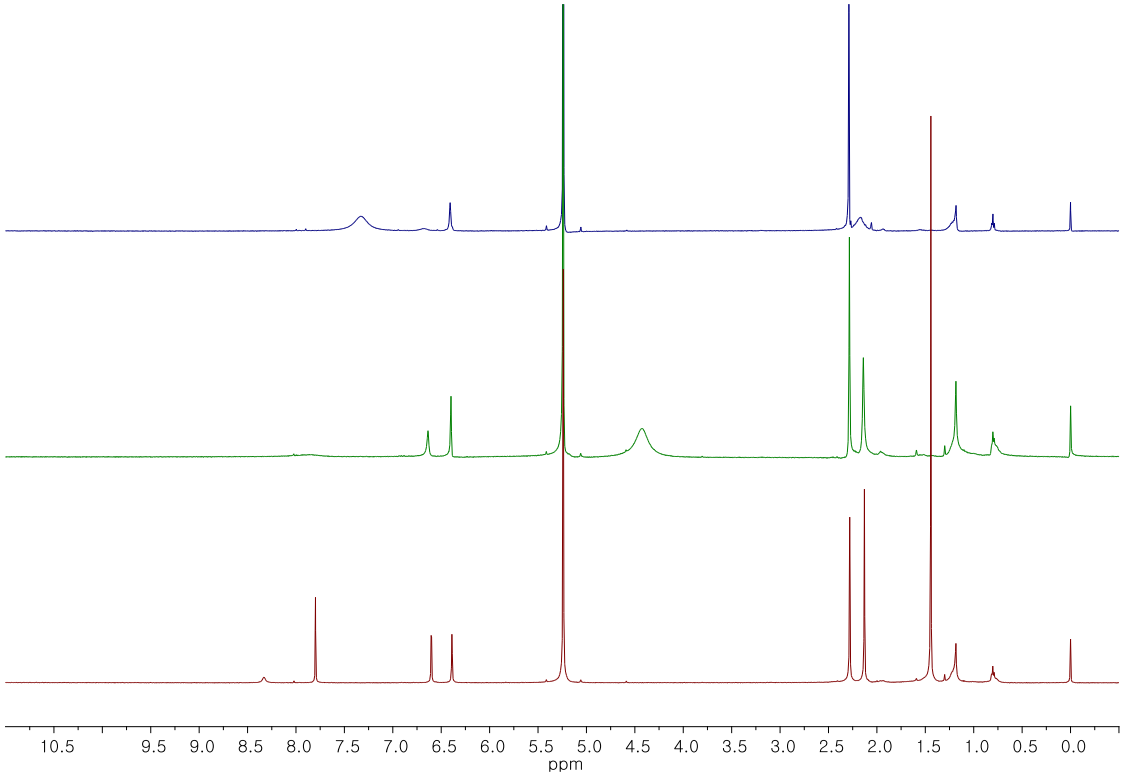

Figure S22. Stacked ^{1}H NMR spectra of 2 mM dichloromethane solutions of **2** obtained via the addition of 0 (bottom), 5 (middle) and 10 (top) equivalents of TFA.

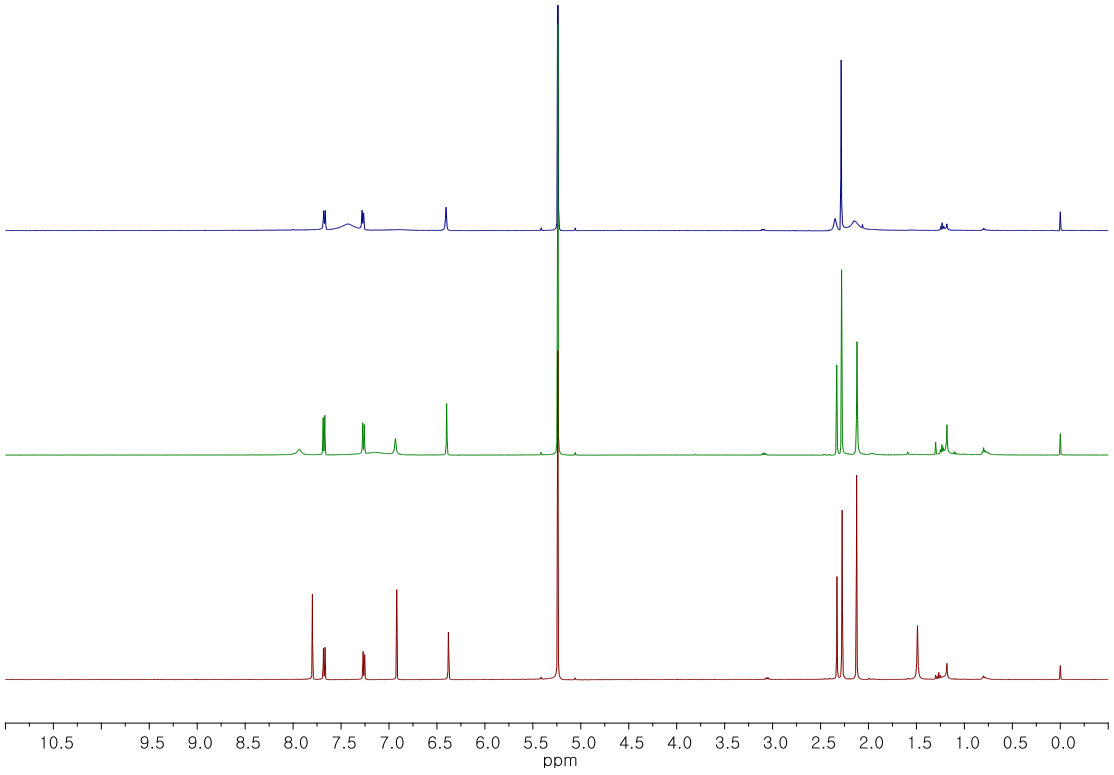

Figure S23. Stacked NMR spectra of 2 mM dichloromethane solutions of **3** obtained via the addition of 0 (bottom), 5 (middle) and 10 (top) equivalents of TFA.

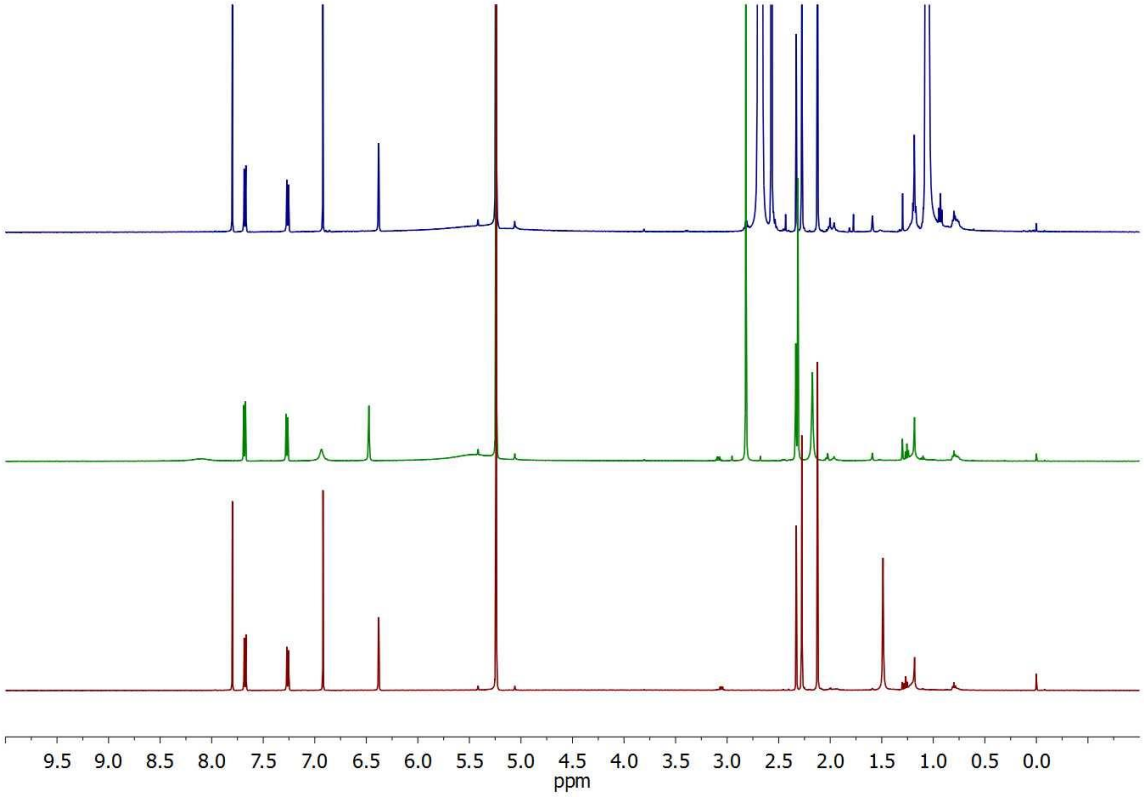

Figure S24. Stacked NMR spectra of 2 mM dichloromethane solutions of **3** obtained via the addition of 0 (bottom), 5 equivalent of MSA (middle) and 20 (top) equivalents of TEA.

VI. EPR Spectral Studies

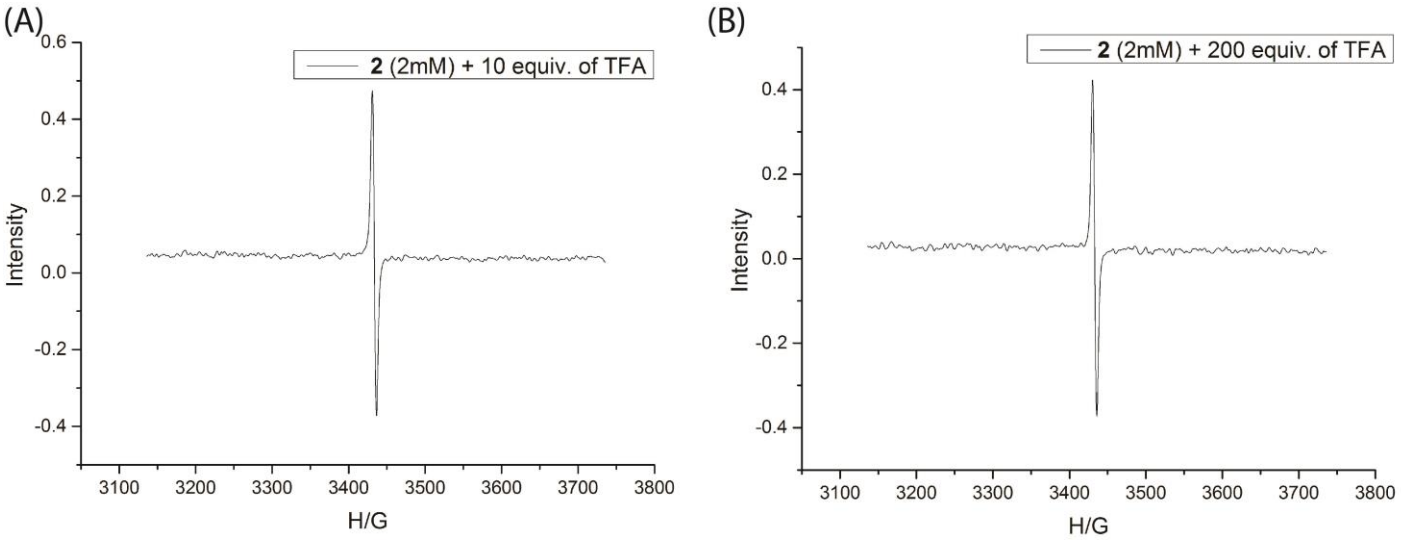

Figure S25. EPR spectra of 20 mM dichloromethane solutions of **2** obtained via the addition of 10 (A) and 200 (B) equivalents of TFA. The spectra were recorded at room temperature.

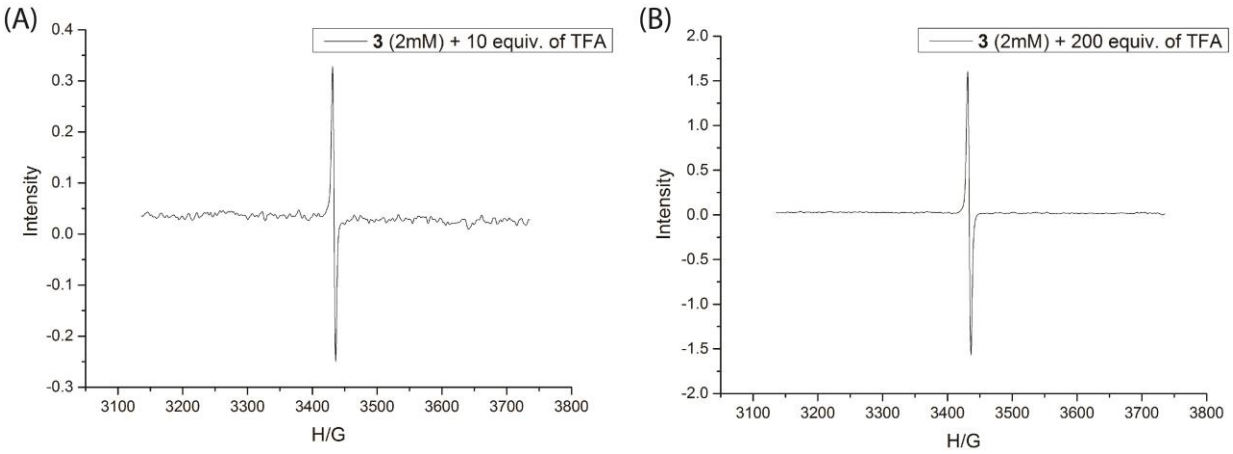

Figure S26. EPR spectra of 2 mM dichloromethane solutions of **3** obtained via the addition of 10 (A) and 200 (B) equivalents of TFA. The spectra were measured at room temperature.

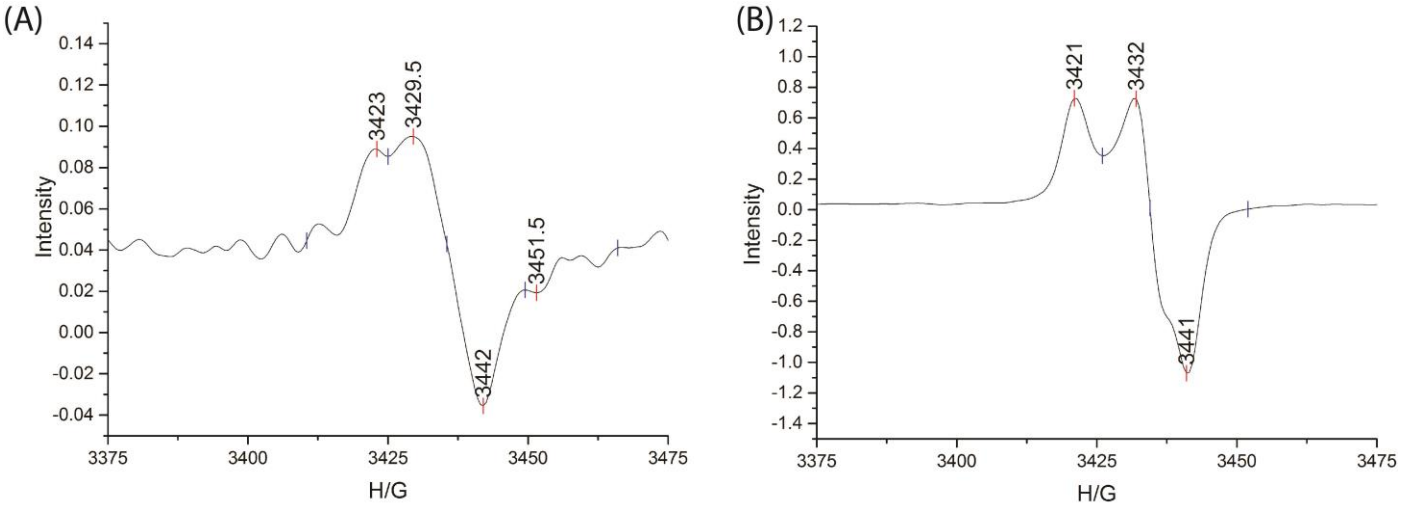

Figure S27. EPR spectra of 2 mM dichloromethane solutions of **2** (left) and **3** (right) recorded at 5K in the presence of 10 equivalents of TFA.

VI. X-ray Crystallographic Analyses

Table S1. Crystal data and structure refinement for **1**, **2**, and **3**•$(CH_3SO_3H)_2$

Parameter	**1**	**2**	**3**•$(MSA)_2$
Chemical formula	$C_{14}H_7N_3S_4$	$C_{26}H_{19}N_3S_6$	C_{36} H_{34} Cl_3 N_3 O_8 S_9
Formula mass	345.47	565.80	1031.55
Crystal system	Monoclinic	Monoclinic	Triclinic
Space group	P 2_1/n	C 2/c	P-1
Crystal color	red	orange	Green
a (Å)	7.2126(3) Å	29.9118(11) Å	10.8535(3) Å
b (Å)	17.1917(7) Å	20.1932(11) Å	12.4996(4) Å
c (Å)	10.7279(5) Å	9.8958(4) Å	18.2429(5) Å
α (deg)	90°	90°	109.3710(12) °
β (deg)	94.846(3)°	102.473(4)°	93.9288(12) °
γ (deg)	90°	90°	103.0890(13) °
Volume (Å^3)	1325.47(10) Å ^{3}	5836.1(5) Å ^{3}	2246.19(11) Å ^{3}
Z	4	8	2
Temperature (K)	170(2) K	192(2) K	223(2) K
θ range	2.24 to 28.33°	2.31 to 26.00°	2.599 to 77.667°
Completeness to θ	97.9%	96.5%	97.8%
Reflections collected / unique	44088/	47517/5542	63643/9367
R_{int}	0.1150	0.1451	0.0656
Absorption correction	multi-scan	multi-scan	multi-scan
Data/restraints/parameters	3234 / 0 / 190	5542 / 0 / 320	9367/0/539
Goodness-of-fit on F^2	1.019	1.010	1.087
Final R indices [I>2δ(I)]	R1 = 0.0661	R1 = 0.0949	R1 = 0.0695
	wR2 = 0.1672	wR2 = 0.2104	wR2 = 0.1990
R indices (all data)	R1 = 0.0996	R1 = 0.1556	R1 = 0.0806
	wR2 = 0.1848	wR2 = 0.2445	wR2 = 0.2310
CCDC number	**1828681**	**1828682**	**1828683**

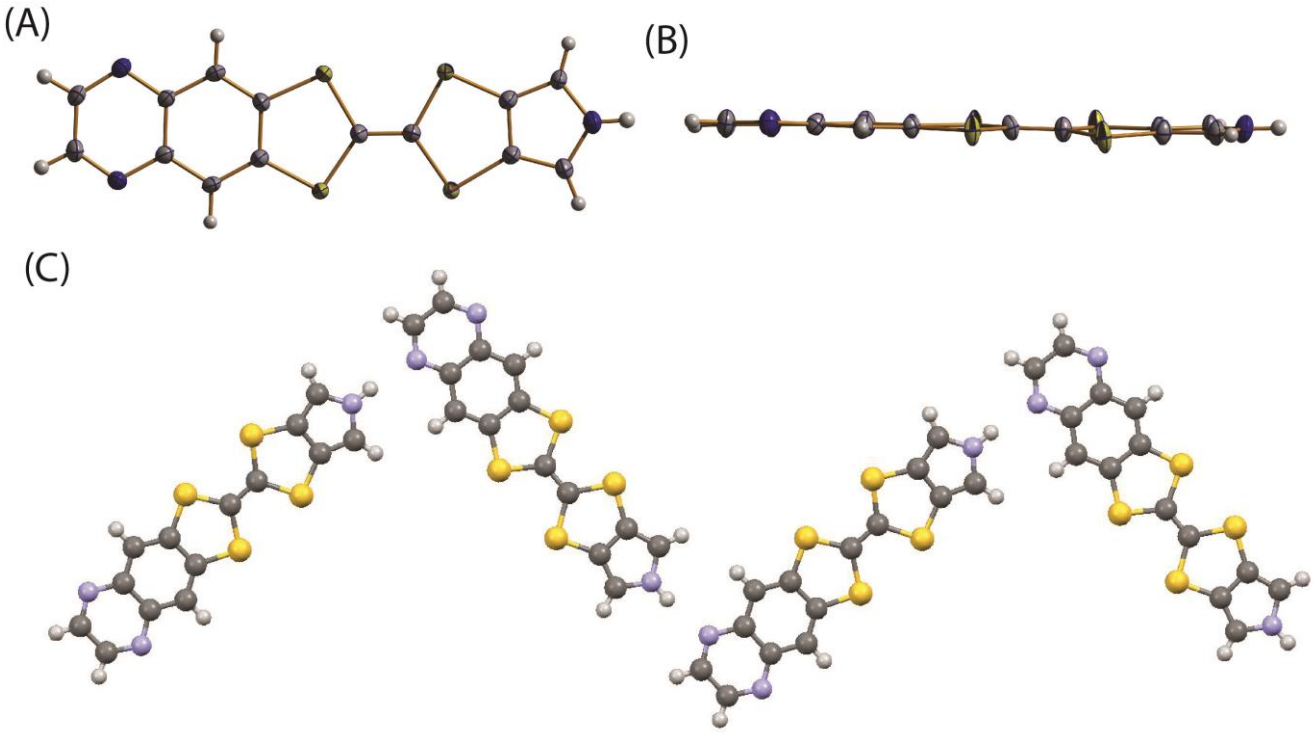

Figure S28. Single crystal X-ray structure **1** (A and B) and its extended structure (C), showing the planar geometry and intermolecular hydrogen bonding interactions, respectively.

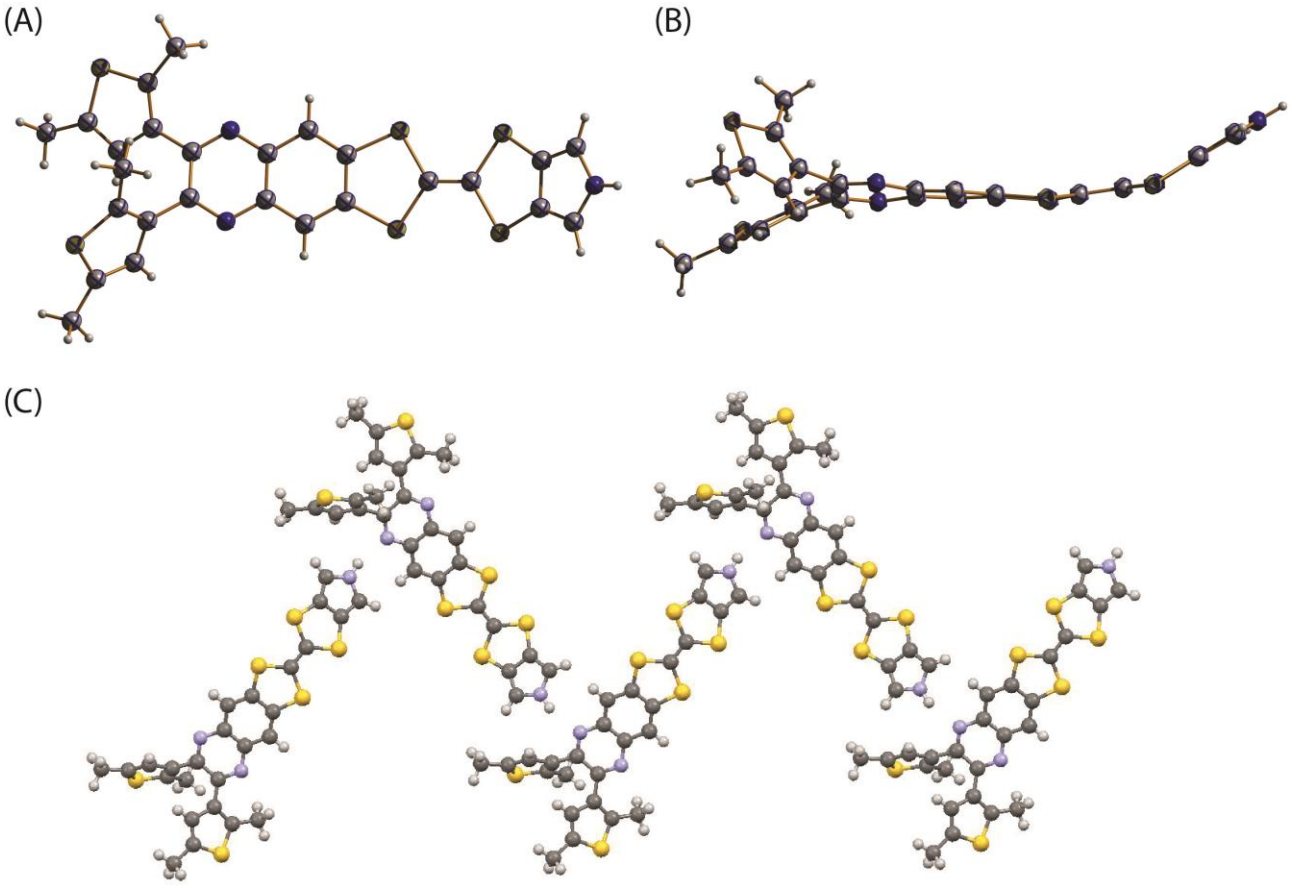

Figure S29. X-ray crystal structure **2** (A and B) and its extended structure (C), showing the bent geometry and intermolecular hydrogen bonding interactions, respectively.

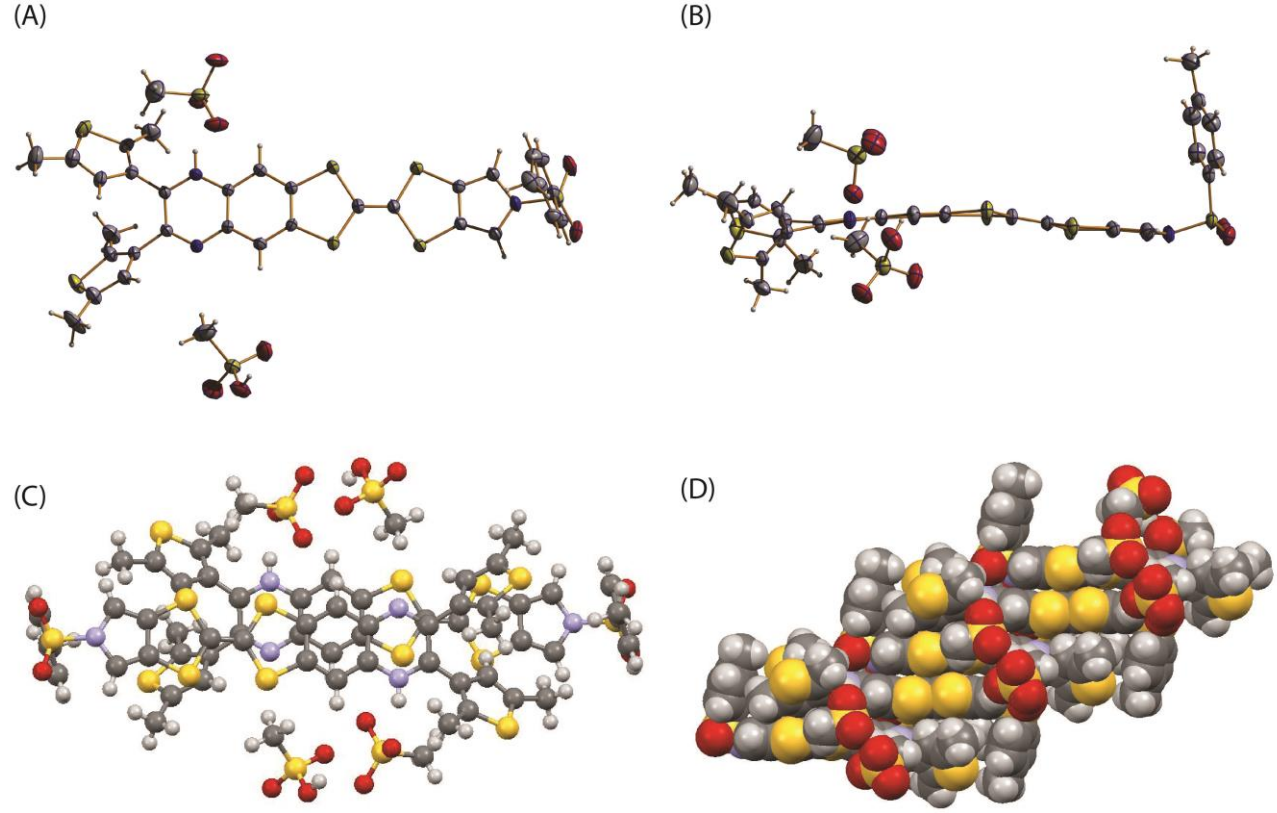

Figure S30. X-ray crystal structure of **3**•$(CH_3SO_3H)_2$ (A and B), showing the planar geometry and its extended structure (C and D) highlighting the intermolecular hydrogen bonding interactions and stacked columnar structure, respectively.

VI. DFT Caluation

The geometry-optimized structures and associated HOMO and LUMO calculations were carried out at the B3LYP 6–31G*(d) level of theory using the commercially available Spartan'10 Window program.

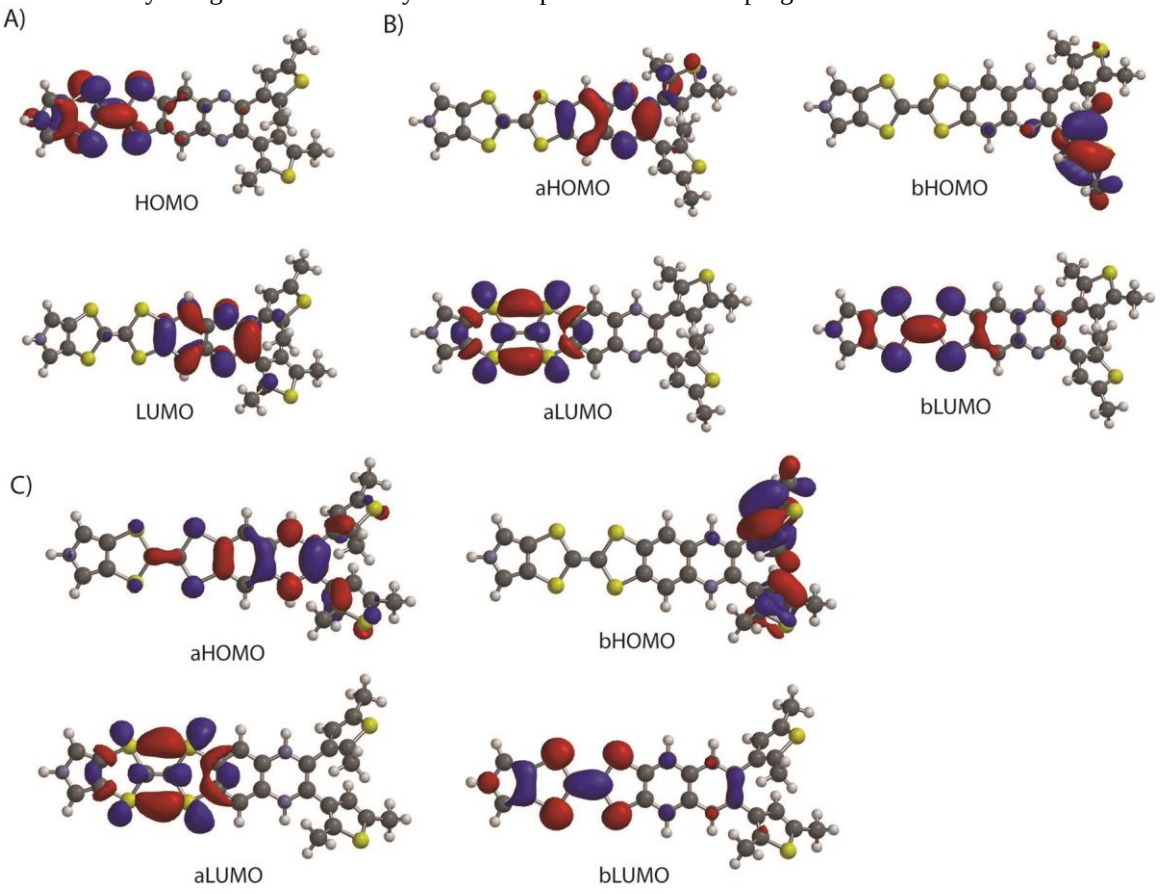

Figure S31. Calculated HOMO/LUMO orbital distributions of neutral (A), monoprotonated (B), and deprotonated (C) forms of the compound **2** .

References for ESI

[1] J. O. Jeppesen, K. Takimiya, F. Jensen, T. Brimert, K. Nielsen, N. Thorup, and J. Becher, *J. Org. Chem*, **2000**, *65*, 5794.
[2] R. Bolligarla, S. N. Reddy, G. Durgaprasad, V. Sreenivasulu, S. K. Das, *Inorg. Chem*., **2013**, *52*, 66.